Syntheses, Structures and Magnetic Properties of Novel Oxamido-Bridged Tetranuclear Complexes [Cu_3M] (M = Cu, Mn)

Shi-bin Wang,[a,b] Guang-ming Yang,*[a] Rong-fang Li,[a] Yuan-fang Wang,[a] and Dai-zheng Liao[a]

Keywords: Oxamido bridge / Tetranuclear / Macrocyclic complex / Magnetic property

Three oxamido-bridged tetranuclear complexes with the formulae [(LCu)Cu(LCuSCN)$_2$]·H_2O (**1**), [(LCu)Mn(LCuSCN)$_2$]·1.38CH_3OH (**2**) and {(LCu)Mn[LCuN(CN)$_2$]$_2$}·0.75DMF·0.25H_2O (**3**) (where H_2L = 2,3-dioxo-5,6:15,16-dibenzo-1,4,8,13-tetraazacylotetradeca-7,13-diene) have been prepared and characterised. Their structures were deduced using X-ray crystallography. All three complexes crystallise in the triclinic system, space group $P\bar{1}$. The three copper ions of the complex ligands and the central metal ions (Cu, Mn) remain in the plane and form a scalene triangle. Three copper ions occupy the vertexes and the M(Cu, Mn) ions are located at the centre. Magnetic susceptibility measurements in the 5–300 K temperature range have been carried out for this series of complexes. The experimental data have been fitted according to the Heisenberg Hamiltonian and led to J values equal to -61.80 cm^{-1}, -14.54 cm^{-1} and -12.10 cm^{-1} for complex **1**, **2** and **3**, respectively. Their interaction parameters have been compared with each other. The deviation of the copper ions from the oxamide-bridge plane results in the J value of complex **1** being different from those of other oxamide-bridged copper complexes.

Introduction

A lot of work has been devoted to the study of the exchange interactions in polynuclear systems. One of the challenges in this field is the design of complexes with predictable magnetic properties. To achieve this goal, one of the best strategies for designing and synthesising complexes is the complex-as-ligand approach, i.e. using mononuclear complexes which contain potential donor groups towards another metal ion.[1−5] The attractive feature of this is that the second metal ion will usually be in a different coordination environment from the first, potentially allowing the facile synthesis of homonuclear complexes in which the metals have different geometries and/or oxidation states,[6−11] or heteronuclear complexes.[12−14] At the same time, it was also discovered that the oxamido group is an efficient bridging mediator of magnetic exchange between neighbouring metal ions[15] because (i) the lower electronegativity of nitrogen with respect to oxygen leads to the gap between the oxamide-bridge molecular orbitals and the d metal orbitals being smaller; (ii) the metal-nitrogen and metal-oxygen distances are very close and contribute to maintaining a good overlap between the bridge and the d-metal orbitals.[16] Many complexes including this bridge have been synthesised and their magnetic properties characterised.[17−21] Antiferromagnetic interactions have been observed in these complexes, the magnitudes of which basically depend upon two factors: one is the nature and magnitude of the overlap between the metal d orbitals containing the unpaired electrons and the bridging ligand orbitals. The other is the energy difference between the two magnetic orbitals.

Polymetallic complexes of macrocyclic ligands have been of great interest to supramolecular and coordination chemists because of their special structures. The macrocyclic oxamido, in which an *exo-cis* conformation of the oxygen donors is enforced, allows us to design heterometallic systems and model magnetic systems in a more controlled fashion via the stepwise complication of the macrocyclic *exo* donors.

With these considerations in mind and continuing our work on polynuclear macrocyclic complexes,[19−25] we designed and synthesised a macrocyclic complex ligand LCu (where H_2L = 2,3-dioxo-5,6:15,16-dibenzo-1,4,8,13-tetraazacylotetradeca-7,13-diene) with oxamido bridging. Based on this complex ligand, we described the syntheses, crystal structures and the magnetic properties of three tetranuclear complexes, namely [(LCu)Cu(LCuSCN)$_2$]·H_2O (**1**), [(LCu)Mn(LCuSCN)$_2$]·1.38CH_3OH (**2**) and [(LCu)Mn[LCuN(CN)$_2$]$_2$]·0.75DMF·0.25H_2O (**3**). Although there have been a few papers concerning tetranu-

---

[a] Department of Chemistry, Nankai University,
Tianjin 300071, People's Republic of China
Fax: (internat.) + 86-22-23502458
E-mail: yanggm@nankai.edu.cn
[b] Department of Materials and Chemical Engineering, Guilin Institute of Technology,
Guilin, People's Republic of China
E-mail: sbinwang@hotmail.com

DOI: 10.1002/ejic.200400253

clear complexes in recent years,[26−32] the structures of the three complexes that we are reporting in this paper are different because the structures of those complexes are square or cubic and little work has been devoted to triangular frameworks in a plane.

Results and Discussion

Description of the Structures

The structure of **1** is shown in Figure 1. It consists of a neutral tetranuclear unit and a large number of disordered waters.

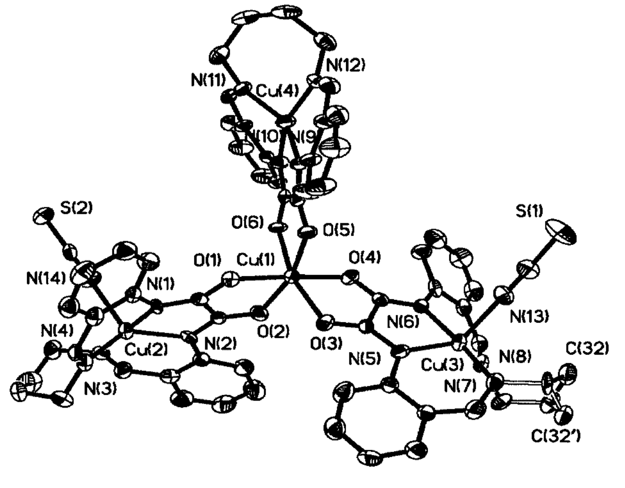

Figure 1. ORTEP plot of **1**; thermal ellipsoids are shown at the 30% probability level

The four copper ions remain in a plane and form a scalene triangle. Cu2, Cu3 and Cu4 occupy the vertexes. Cu1 almost stands on the epicenter since its distances to Cu2, Cu3 and Cu4 are 5.21(2) Å, 5.25 (1) Å and 5.23(2) Å, respectively. The Cu ions deviate from the mean triangular plane by 0.0114(3) Å (Cu1), −0.0040(2) Å (Cu2), −0.0042(2) Å (Cu3) and −0.0032 (1) Å (Cu4). In this molecule, there are three coordination frameworks to every four copper ions. The Cu1 ion is connected to other copper ions via the *exo-cis* oxygen atoms of the oxamido macrocyclic ligands and its coordination polyhedron can be considered as a distorted octahedron. The basal plane of the octahedron consists of O1, O2, O4 and O5 and the apical positions are occupied by O3 and O6. The value that Cu1 deviates from the plane is 0.0463 Å. Cu2 and Cu3 show a (4+1) coordination environment, the four nitrogen atoms of the macrocyclic ligand are situated in the basal position and the coordination is completed by the nitrogen of the SCN^-. The four nitrogen atoms of the macrocyclic ligand deviate significantly from the basal plane [for Cu2, the values are −0.41(2) Å (N1), 0.41 (3) Å (N2), −0.36 (2) Å (N3) and 0.37 (1) Å (N4)]. The coordination environment of Cu2 can be considered as a square pyramid. The Cu−N bond lengths in the plane range from 1.912(1) Å to 1.973 (3) Å for Cu2 and from 1.891(1) Å to 1.995 (3) Å for Cu3. The axial Cu−N bond length is 2.107(1) Å for Cu2 and 2.081 (3) Å for Cu3. These are elongated due to the Jahn−Teller effect of the d^9 electronic configuration. For Cu4, the four-coordinate structure of the complex ligand is maintained. Cu2, Cu3 and Cu4 deviate from the plane of the oxamido bridge ($C_2O_2N_2$) by −0.274(4) Å, 0.166 (1) Å and 0.0457 (1) Å, respectively. Figure 1 indicates that C32 is disordered over two sides.

Complexes **2** and **3** are similar in structure and both consist of a neutral tetranuclear Cu_3Mn unit. Figures 2 and 3 show the common metal part of **2** and **3** with atomic labelling schemes. Within each tetranuclear fragment the Cu1 and Cu2 centres of **2** and the Cu2 and Cu3 centres of **3** are in a (4+1) coordination environment and show square pyramidal structures. The four nitrogen atoms of the macrocyclic ligand form their basal planes and the axial positions are occupied, respectively, by the nitrogen atom from thiocyanate ion for complex **2** and one of the nitrogen atoms of the dicyanamide ion for complex **3**. The Cu3 centre of complex **2** and Cu1 in complex **3** both maintain the four-coordinate structure of the macrocyclic complex ligand. The four copper ions which have pentahedral configurations in these two complexes are displaced from the least-squares basal plane towards the apical ligand by 0.36 (1) Å (Cu1) and 0.47(3) Å (Cu2) for complex **2** and by −0.31(2) Å (Cu2) and 0.39(1) Å (Cu3) for complex **3**. The metal atoms Cu1, Cu2, Cu3 and Mn1 of the two complexes are almost in a plane and form a triangle. The Mn(ii) ions in the two complexes are both coordinated to the six oxygen atoms of the oxamido bridges of the three complex ligands. The Mn(ii) ions have octahedral geometries and the Mn−O bond lengths range from 2.152(1) Å to 2.179(1) Å for complex **2** and from 2.094 (2) Å to 2.187 (3) Å for complex **3**. The distances from Mn to Cu are 5.514(2) Å (Cu1), 5.547(2) Å (Cu2) and 5.461(2) Å (Cu3) for complex **2** and 5.433 (1) Å (Cu1), 5.441(1) Å (Cu2) and 5.485 (1) Å (Cu3) for complex **3**, respectively. There are many free solvent molecules in both crystal structures. On average, there are 1.38 methanol molecules in the crystalline lattice of complex **2**. However, 0.75 DMF molecules and 0.25 water molecules are distributed in the crystalline lattice of complex **3**.

Selected bond lengths and angles are listed in Tables 1, 2 and 3.

Spectroscopic Characterisation

The $\nu_{(C=O)}$ bands of the oxamido group of the tetranuclear complexes can be observed around 1640cm^{-1} which is lower relative to that of mononuclear CuL (1670cm^{-1}). The IR bands around 1570cm^{-1} can be assigned to the $\nu_{(C=N)}$ mode of the macrocycle. A strong band at ca. 2100cm^{-1} is characteristic of a C−N bond.

The electronic absorption spectra of the three tetranuclear complexes in DMF below 420 nm are dominated by intense bands due to intraligand and charge-transfer transitions in the Cu(ii) chromophore. Bands at 670 nm can be attributed to the spin allowed d-d transitions of Cu(ii). The coordination environments of manganese in 2 and 3 are distorted octahedral. Thus, according to ligand field theory

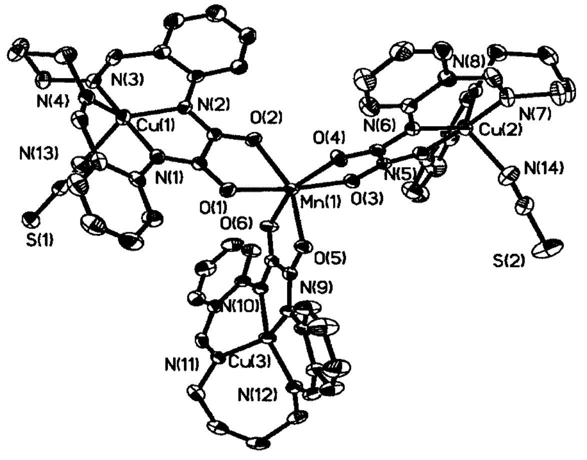

Figure 2. ORTEP plot of **2**; thermal ellipsoids are shown at the 30% probability level

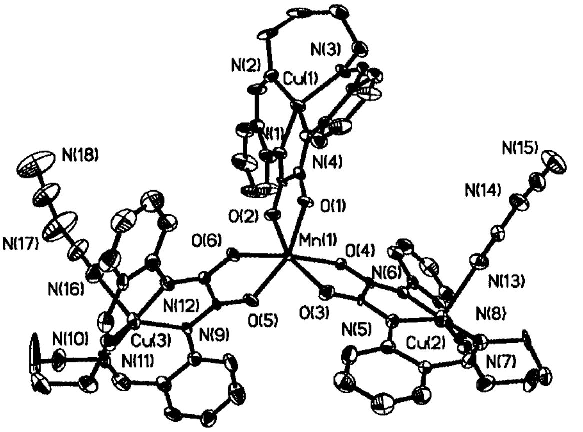

Figure 3. ORTEP plot of **3**; thermal ellipsoids are shown at the 30% probability level

and assuming O_h symmetry, the ground state of manganese is $^6A_{1g}$. Because d-d transitions of manganese [$^6A_{1g}\rightarrow{}^4T_{1g}(G)$. $^4T_{2g}(G)$, $^4A_{1g}$ ···] are spin forbidden, no characteristic bands of manganese were found in the spectra of the complexes.

Magnetic Properties

Table 1. Selected bond lengths (Å) and angles (°) in **1**

Cu(1)−O(4)	1.883(6)	Cu(2)−N(14)	2.107(9)
Cu(1)−O(1)	1.900(6)	Cu(3)−N(7)	1.995(7)
Cu(1)−O(5)	2.030(6)	Cu(3)−N(13)	2.081(9)
Cu(1)−O(2)	2.064(6)	Cu(3)−N(8)	1.891(8)
Cu(1)−O(6)	2.061(6)	Cu(3)−N(6)	1.903(7)
Cu(1)−O(3)	2.117(7)	Cu(4)−N(12)	1.896(7)
Cu(2)−N(1)	1.924(7)	Cu(4)−N(9)	1.898(8)
Cu(2)−N(2)	1.959(7)	Cu(4)−N(10)	1.901(7)
Cu(2)−N(4)	1.973(8)	Cu(4)−N(11)	1.911(8)
O(4)−Cu(1)−O(1)	176.8(2)	N(3)−Cu(2)−N(4)	93.9(3)
O(4)−Cu(1)−O(5)	95.3(3)	N(1)−Cu(2)−N(4)	89.9(3)
O(1)−Cu(1)−O(5)	86.9(2)	N(2)−Cu(2)−N(4)	133.1(3)
O(4)−Cu(1)−O(2)	98.2(2)	N(3)−Cu(2)−N(14)	91.0(3)
O(1)−Cu(1)−O(2)	79.9(2)	N(1)−Cu(2)−N(14)	89.7(3)
O(5)−Cu(1)−O(2)	164.7(2)	N(2)−Cu(2)−N(14)	120.9(3)
O(4)−Cu(1)−O(6)	87.6(3)	N(4)−Cu(2)−N(14)	105.5(3)
O(1)−Cu(1)−O(6)	95.1(2)	N(8)−Cu(3)−N(7)	92.1(3)
O(5)−Cu(1)−O(6)	79.2(2)	N(6)−Cu(3)−N(7)	89.0(3)
O(2)−Cu(1)−O(6)	94.1(2)	N(5)−Cu(3)−N(7)	131.2(3)
O(4)−Cu(1)−O(3)	79.1(3)	N(8)−Cu(3)−N(13)	93.4(3)
O(6)−Cu(1)−O(3)	164.4(2)	N(6)−Cu(3)−N(13)	90.0(3)
O(1)−Cu(1)−O(3)	98.4(3)	N(5)−Cu(3)−N(13)	118.4(3)
O(5)−Cu(1)−O(3)	93.7(3)	N(7)−Cu(3)−N(13)	109.7(3)
O(2)−Cu(1)−O(3)	95.8(3)	N(9)−Cu(4)−N(10)	85.5(3)
N(3)−Cu(2)−N(1)	175.8(3)	N(12)−Cu(4)−N(11)	98.9(3)
N(3)−Cu(2)−N(2)	92.2(3)	N(9)−Cu(4)−N(11)	150.9(3)
N(1)−Cu(2)−N(2)	83.9(3)	N(10)−Cu(4)−N(11)	92.5(3)

Table 2. Selected bond lengths (Å) and angles (°) in **2**

Cu(1)−N(3)	1.949(5)	Cu(2)−N(6)	2.030(4)
Cu(1)−N(1)	1.961(4)	Cu(2)−N(8)	2.058(4)
Cu(1)−N(2)	2.011(4)	Cu(2)−N(14)	2.111(6)
Cu(1)−N(4)	2.024(4)	Cu(3)−N(10)	1.945(4)
Cu(1)−N(13)	2.196(5)	Cu(3)−N(12)	1.962(4)
Cu(2)−N(5)	1.954(4)	Cu(3)−N(11)	1.966(4)
Cu(2)−N(7)	1.967(4)	Cu(3)−N(9)	1.972(4)
Mn(1)−O(3)	2.151(3)	Mn(1)−O(1)	2.171(3)
Mn(1)−O(5)	2.151(3)	Mn(1)−O(2)	2.178(3)
Mn(1)−O(6)	2.160(3)	Mn(1)−O(4)	2.195(3)
N(1)−Cu(1)−N(2)	83.94(16)	N(5)−Cu(2)−N(14)	91.09(19)
N(3)−Cu(1)−N(4)	93.38(19)	N(7)−Cu(2)−N(14)	93.4(2)
N(1)−Cu(1)−N(4)	91.25(18)	N(6)−Cu(2)−N(14)	117.96(18)
N(2)−Cu(1)−N(4)	135.77(16)	N(8)−Cu(2)−N(14)	112.15(18)
N(3)−Cu(1)−N(13)	91.02(18)	N(10)−Cu(3)−N(12)	161.14(16)
N(1)−Cu(1)−N(13)	88.12(17)	N(10)−Cu(3)−N(11)	92.69(17)
N(2)−Cu(1)−N(13)	120.03(16)	N(12)−Cu(3)−N(11)	97.94(17)
N(4)−Cu(1)−N(13)	103.64(17)	N(10)−Cu(3)−N(9)	85.36(17)
N(5)−Cu(2)−N(7)	175.09(18)	N(12)−Cu(3)−N(9)	93.35(17)
N(5)−Cu(2)−N(6)	83.16(16)	N(11)−Cu(3)−N(9)	148.77(16)
N(7)−Cu(2)−N(6)	92.99(17)	O(6)−Mn(1)−O(2)	96.06(13)
N(5)−Cu(2)−N(8)	88.04(17)	O(3)−Mn(1)−O(5)	99.72(13)
O(5)−Mn(1)−O(6)	75.77(12)	O(3)−Mn(1)−O(6)	89.18(13)
O(3)−Mn(1)−O(1)	173.21(12)	O(3)−Mn(1)−O(4)	74.12(12)
O(5)−Mn(1)−O(1)	85.81(13)	O(5)−Mn(1)−O(4)	95.63(13)
O(6)−Mn(1)−O(1)	96.04(13)	O(6)−Mn(1)−O(4)	159.84(13)
O(3)−Mn(1)−O(2)	100.59(13)	O(1)−Mn(1)−O(4)	101.55(13)
O(5)−Mn(1)−O(2)	157.97(12)	O(2)−Mn(1)−O(4)	98.05(14)
O(1)−Mn(1)−O(2)	74.59(13)		

Variable temperature (5−300 K) magnetic susceptibility data were collected for microcrystalline samples of complexes **1−3** in a magnetic field of 10000 G. The χ_M and $\chi_M T$ versus T plot for complex **1** is shown in Figure 4. At 300 K $\chi_M T$ is equal to 1.35cm^{3}mol^{-1}K which is lower than that expected for the four isolated copper ions ($\chi_M T$ = 1.50 cm^{3}mol^{-1}K). This decreases smoothly upon cooling and reaches a minimum at about 70 K with $\chi_M T$ = 1.05cm^{3}mol^{-1}K and increases upon cooling further. At 5 K, $\chi_M T$ is equal to 1.30 cm^{3}mol^{-1}K. The experimental data were fitted using the theoretical expression of the magnetic susceptibility [Equation (1)] which was deduced from the spin Hamiltonian:

Table 3. Selected bond lengths (Å) and angles (°) in **3**

Mn(1)−O(4)	2.092(7)	Cu(2)−N(13)	2.318(12)
Mn(1)−O(6)	2.098(7)	Cu(2)−N(8)	1.956(10)
Mn(1)−O(1)	2.148(7)	Cu(2)−N(6)	1.966(9)
Mn(1)−O(2)	2.146(7)	Cu(2)−N(5)	2.009(8)
Mn(1)−O(3)	2.159(7)	Cu(2)−N(7)	2.025(10)
Mn(1)−O(5)	2.187(7)	Cu(3)−N(9)	2.023(8)
Cu(1)−N(2)	1.952(9)	Cu(3)−N(12)	1.947(9)
Cu(1)−N(4)	1.961(9)	Cu(3)−N(10)	1.975(9)
Cu(1)−N(3)	1.969(9)	Cu(3)−N(11)	2.035(10)
Cu(1)−N(1)	1.972(9)	Cu(3)−N(16)	2.195(12)
O(6)−Mn(1)−O(1)	88.4(3)	N(2)−Cu(1)−N(3)	99.6(4)
O(4)−Mn(1)−O(2)	86.8(3)	N(4)−Cu(1)−N(3)	91.4(4)
O(6)−Mn(1)−O(2)	98.0(3)	N(2)−Cu(1)−N(1)	93.3(4)
O(1)−Mn(1)−O(2)	76.5(3)	N(4)−Cu(1)−N(1)	85.2(4)
O(4)−Mn(1)−O(3)	76.0(3)	N(3)−Cu(1)−N(1)	148.5(4)
O(6)−Mn(1)−O(3)	99.9(3)	N(8)−Cu(2)−N(6)	174.0(4)
O(1)−Mn(1)−O(3)	95.6(3)	N(8)−Cu(2)−N(5)	92.3(4)
O(2)−Mn(1)−O(3)	160.1(3)	N(6)−Cu(2)−N(5)	84.3(4)
O(4)−Mn(1)−O(5)	99.7(3)	N(8)−Cu(2)−N(7)	95.0(4)
O(6)−Mn(1)−O(5)	75.5(3)	N(6)−Cu(2)−N(7)	90.7(4)
O(1)−Mn(1)−O(5)	160.1(3)	N(5)−Cu(2)−N(7)	140.1(4)
O(2)−Mn(1)−O(5)	94.1(3)	N(8)−Cu(2)−N(13)	89.3(4)
N(6)−Cu(2)−N(13)	87.8(4)	N(10)−Cu(3)−N(11)	94.1(4)
N(5)−Cu(2)−N(13)	115.7(4)	N(9)−Cu(3)−N(11)	135.1(4)
N(7)−Cu(2)−N(13)	103.6(4)	N(12)−Cu(3)−N(16)	89.4(4)
N(12)−Cu(3)−N(10)	176.6(4)	N(10)−Cu(3)−N(16)	92.3(4)
N(12)−Cu(3)−N(9)	83.6(4)	N(9)−Cu(3)−N(16)	115.5(4)
N(10)−Cu(3)−N(9)	93.0(4)	N(11)−Cu(3)−N(16)	108.4(4)
N(12)−Cu(3)−N(11)	88.2(4)		

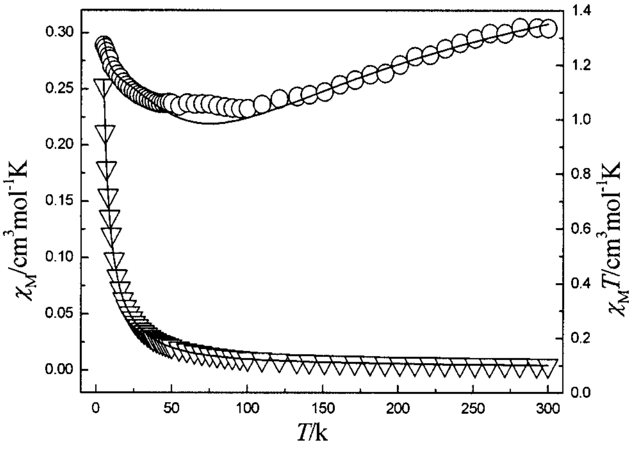

Figure 4. Experimental and calculated variations of the product χ_M and $\chi_M T$ versus T for **1**

$$\chi_M = \frac{2Ng^2\beta^2}{k(T-\theta)}\left[\frac{A}{B}\right] + N\alpha$$

$$A = 5\times\exp(2J/kT) + \exp(-2J/kT) + 2 \tag{1}$$

$$B = 5\times\exp(2J/kT) + 3\times\exp(-2J/kT) + 2\times\exp(-2J/kT) + 6$$

where J is the exchange integral between the Cu(II) ions. (Because Cu2, Cu3 and Cu3 all link to Cu1 through the oxamido bridge and the distances between them are almost similar, we assumed the interaction between them is equal.) $N\alpha$ is the temperature-independent paramagnetic (240×10^{-6} cm^{3}mol^{-1}) and the other symbols have their usual meanings. The best fitting of the experimental data leads to $J = -61.80\text{cm}^{-1}$, $g = 2.09$, $\theta = 0.8$ and $R = 2.23 \times 10^{-4}$ (R is the agreement factor defined as $\Sigma(\chi_{\text{obs.}} - \chi_{\text{calcd.}})^2/\Sigma\chi^2_{\text{obs.}}$). The results indicate that there is an antiferromagnetic interaction between the copper(II) ions within complex **1**.

According to the Kahn model[33] for the copper complexes, the magnetic exchange pathway is dominated by the interaction between the metal $x^2 - y^2$ orbitals and the oxamido σ orbitals and the antiferromagnetic interaction between the copper(II) ions arises from the nonzero overlap between the magnetic orbitals. The magnitude of the antiferromagnetic interaction is related to the square of the overlap between the magnetic orbitals central to each copper. The antiferromagnetic interaction between the copper(II) ions within complex **1** is weaker than that within other oxamido bridge copper complexes reported previously ($J = 210-80.9$ cm^{-1}).[34−36] This may be attributed to the difference in the ligand environments of the copper ions because the former has less co-planarity between the coordination environments of copper(II) and that of the adjacent copper(II) ions than the latter, resulting in a decrease in overlap between the two magnetic orbitals within the present complex.[37]

Plots of χ_M and $\chi_M T$ versus temperature for complexes **2** and **3** are shown in Figures 5 and 6, respectively. At room temperature, $\chi_M T$ is equal to 5.04 cm^{3}mol^{-1}K for complex **2** and 5.19 cm^{3}mol^{-1}K for complex **3**, both of which are lower than 5.50 cm^{3}mol^{-1}K which would be expected for noninteracting ions [three coppers(II) ions and one manganese(II) ion]. The $\chi_M T$ value decreases steadily upon cool-

$$\chi_M = \frac{N\beta^2}{kT}\left[\frac{A}{B}\right] + N\alpha$$

$$A = 60\times g^2_{4,3/2}\times\exp(18J/kT) + 28\times g^2_{3,3/2}\times\exp(4J/kT) + 10\times g^2_{2,3/2}\times\exp(4J/kT) + 2\times g^2_{1,3/2} + 56\times g^2_{3,1/2}\times\exp(13J/kT) + 20\times g^2_{2,1/2}\times\exp(7J/kT)$$

$$B = 9\times\exp(18J/kT) + 7\times\exp(10J/kT) + \exp(4J/kT) + 3 + 14\times\exp(13J/kT) + 10\times\exp(7J/kT) \tag{2}$$

$$g_{4,3/2} = \frac{3}{8}\times g_{Cu} + \frac{5}{8}\times g_{Mn} \qquad g_{3,3/2} = \frac{7}{24}\times g_{Cu} + \frac{17}{24}\times g_{Mn}$$

$$g_{2,3/2} = \frac{1}{12}\times g_{Cu} + \frac{13}{12}\times g_{Mn} \qquad g_{1,3/2} = \frac{-3}{4}\times g_{Cu} + \frac{7}{4}\times g_{Mn}$$

$$g_{3,1/2} = \frac{1}{6}\times g_{Cu} + \frac{5}{6}\times g_{Mn} \qquad g_{2,1/2} = \frac{-1}{6}\times g_{Cu} + \frac{7}{6}\times g_{Mn}$$

ing, showing that an antiferromagnetic interaction between the copper and manganese ions occurs. In the 5−15 K temperature range the $\chi_M T$ plot exhibits a plateau at 1.03 $cm^3 mol^{-1} K$ for complex **2** and at 0.96 $cm^3 mol^{-1} K$ for complex **3**. The experimental data were fitted using the theoretical expression of the magnetic susceptibility [Equation (2)] which was deduced from spin the Hamiltonian: In Equation (2), the value of $N\alpha$ is 180×10^{-6}.

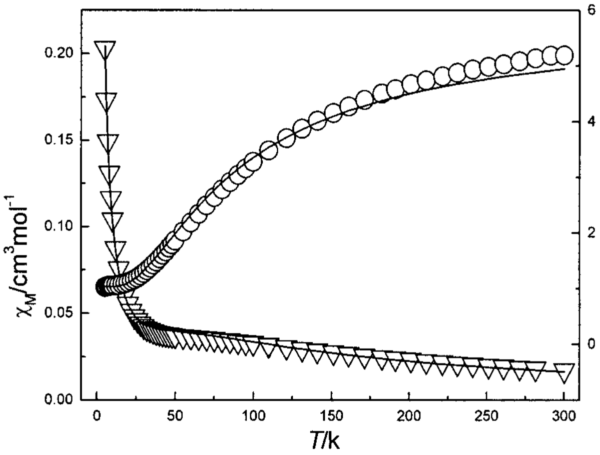

Figure 5. Experimental and calculated variations of the product χ_M and $\chi_M T$ versus T for **2**

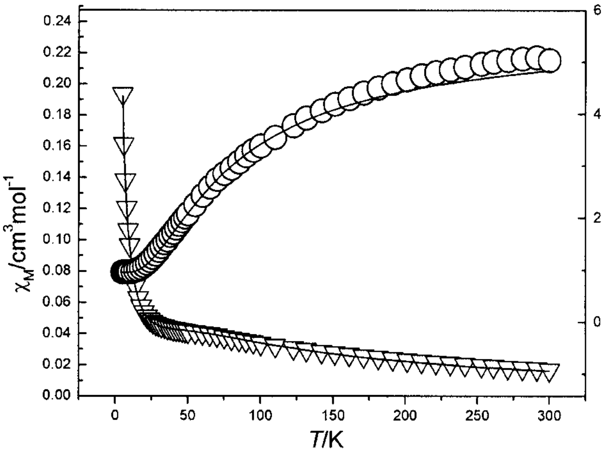

Figure 6. Experimental and calculated variations of the product χ_M and $\chi_M T$ versus T for **3**

The best fit of the data was obtained with the following parameters $J = -14.63\ cm^{-1}$, $g_{Cu} = 2.06$, $g_{Mn} = 1.99$ and $R = 1.05 \times 10^{-3}$ for complex **2** and $J = -12.22 cm^{-1}$, $g_{Cu} = 2.06$, $g_{Mn} = 1.98$ and $R = 1.20 \times 10^{-4}$ for complex **3**. The J values of 2 and 3 are in the range of other reported complexes[16,24] with similar structures.

If we compare the J value of complex **1** with those of complexes **2** and **3**, we see that the latter values are lower than the former. The difference may be attributed to the following reasons: (i) the M−O distance is larger for Mn (2.17 Å) than for Cu (2.01Å) or (ii) the energies of the 3d orbitals of Mn(II) are higher than the corresponding ones in Cu(II). The two factors lead to less delocalisation of the d electron towards the oxamido bridge in **2** and **3** than in complex 1, therefore decreasing the antiferromagnetic interaction in **2** and **3**.[38]

Conclusion

By using the macrocyclic oxamido-copper complex as a complex ligand and SCN^{-1} or $N(CN)^{-1}$ as auxiliary ligands, three novel oxamide-bridge tetranuclear complexes have been obtained. In all complexes, the Cu atoms lie at the apexes of a triangle with the M atom located in the plane and at the centre of this triangle. All attempts to crystallise these types of complexes without smaller ions such as SCN^{-1} and $N(CN)^{-1}$ have previously been unsuccessful. It has been confirmed that the smaller ions can make the crystals grow easily in the present systems. Furthermore, we analysed the variable temperature magnetic susceptibilities of the three complexes. The results indicate that there are antiferromagnetic interactions between metal ions in the complexes. We are attempting to replace the metal ion in the centre of the triangle with a diamagnetic ion in order to research further the spin frustration.

Experimental Section

Physical Measurements: Elemental analyses (C, H, N) were performed on a Perkin−Elmer 240 analyser. IR spectra were recorded on a Shimadzu IR spectrometer as KBr pellets. Variable-temperature magnetic susceptibilities from 5−300 K were measured on a Quantum Design MPMS-7 SQUID magnetometer. Diamagnetic corrections were made with Pascal's constants for all the constituent atoms. The electronic absorption spectra were recorded on a JASCO V-5700 spectrometer.

Caution! Perchlorate salts are potentially explosive and should only be handled in small quantities only.

All starting materials were obtained from commercial suppliers and were of AR grade and were used without further purification. The mononuclear precursors were synthesised using the methods reported previously.[12,38]

Preparation of the Complexes: All complexes were prepared using the same method which is described in detail here using $[(LCu)Cu(LCuSCN)_2]\cdot H_2O$ (**1**) as an example. Copper perchlorate (0.2 mmol, 0.0730 g) dissolved in methanol (5 mL) was added to a DMF solution (25 mL) of LCu (0.7 mmol, 0.2860 g). An aqueous solution (5 mL) of KSCN (0.3 mmol, 0.030 g) was then added dropwise to this mixture. After heating to reflux for 2 hours, the resultant green solution was cooled and filtered and the filtrate was allowed to stand for one month until deep green crystals suitable for X-ray analysis separated out. Yield 40%. $C_{62}H_{59}Cu_4N_{14}O_7S_2$ (1430.51): calcd. C 52.12, H 3.92, N 13.73; found C 52.08, H 4.10, N 13.85. IR (KBr): $\tilde{\nu}$ = 2065 (C−N), 1675 (C=O), 1599 (C=O), 1557 cm^{-1}.

$[(LCu)Mn(LCuSCN)_2]\cdot 1.38CH_3OH$ (2): This complex was obtained following the procedure described above for $[Cu_4]$ except that Cu perchlorate was substituted with Mn perchlorate. The solution was left undisturbed and well-formed grey crystals were obtained after about a month. The yield was ca. 54%.

Table 4. Crystallographic data for complexes **1**, **2** and **3**

	1	**2**	**3**
Empirical formula	$C_{62}H_{59}Cu_4N_{14}O_7S_2$	$C_{63.38}H_{59.50}Cu_3MnN_{14}O_{7.38}S_2$	$C_{66.25}H_{59.75}Cu_3MnN_{18.75}O_7$
Molecular mass	1430.51	1444.93	1476.14
Temperature	293(2) K	293(2) K	293(2) K
Wavelength	0.71073 Å	0.71073 Å	0.71073 Å
Crystal system, space group	triclinic, $P\bar{1}$	triclinic, $P\bar{1}$	triclinic, $P\bar{1}$
Unit cell dimensions			
a (Å)	13.960(11)	13.976(4)	14.349(8)
b (Å)	16.051(13)	16.458(5)	16.395(9)
c (Å)	16.773(12)	17.743(6)	17.402(10)
α (°)	103.024(15)	104.775(6)	102.323(10)
β (°)	107.071(15)	106.467(6)	106.740(10)
γ (°)	108.467(14)	107.267(6)	108.975(10)
Volume (Å^3)	3191(4)	3471.6(19)	3488(3)
Z	2	2	2
Density (mg·m^{-3})	1.489	1.382	1.406
Absorption coeff. (mm^{-1})	1.444	1.204	1.144
F(000)	1466	1482	1513
Crystal size (mm)	0.30 × 0.20 ×0.10	0.30 × 0.24 × 0.20	0.35 × 0.30 × 0.30
θ range for data collection	1.67 to 25.03°	1.66 to 26.44°	1.63 to 25.03°
Data/restraints/parameters	10522/0/811	13938/22/841	11901/38/892
Goodness-of-fit on F^2	0.951	0.988	1.021
Final R indices	$R1 = 0.0750$	$R1 = 0.0596$	$R1 = 0.1017$
[$I > 2\sigma(I)$]	$wR2 = 0.1612$	$wR2 = 0.1155$	$wR2 = 0.2061$
R indices (all data)[a]	$R1 = 0.1797$	$R1 = 0.1456$	$R1 = 0.2386$
	$wR2 = 0.2062$	$wR2 = 0.1484$	$wR2 = 0.2780$
Largest diff. peak and hole e·Å^{-3}	1.084 and −0.540	0.612 and −0.421	1.198 and −0.642

[a] $R = \Sigma|F_o| - |F_c|/\Sigma|F_o|$ $wR = [\Sigma w(F_o{}^2 - F_c{}^2)^2/\Sigma w(F_o{}^2)^2]^{1/2}$

$C_{63.38}H_{59.50}Cu_3MnN_{14}O_{7.38}S_2$ (1444.93): C 52.60, H 4.11, N 13.57; found C 53.64, H 4.17, N 13.69. IR (KBr): $\tilde{\nu}$ = 2066 (C−N), 1636 (C=O), 1601 (C=N), 1576 cm^{-1}.

[(LCu)Mn[LCuN(CN)$_2$]$_2$]·0.75DMF·0.25H$_2$O (3): This compound was obtained by using the method used to synthesise complex **2** except that KSCN was substituted with NaN(CN)$_2$. The crystals were also grey. Yield 47%. $C_{66}H_{60.50}N_{18.50}O_{7.50}Cu_3Mn$ (1476.14) : calcd. C 53.86, H 4.04, N 17.79; found C 53.02, H 4.21, N 17.45. IR (KBr): $\tilde{\nu}$ = 2148 (C−N), 1636 (C=O), 1600 (C=N), 1558 cm^{-1}.

X-ray Data Collections and Structure Determinations

Complex 1: A dark green crystal (0.30 × 0.20 × 0.10 mm) was selected and coated with epoxy resin and mounted on a glass fibre for X-ray data collection. Intensity data were colleted on a BRUKER SMART 1000 diffractometer, using Mo-K_α (λ = 0.71073 Å) radiation. The unit cell constants were determined from a least-squares fit of the setting angles for 25 reflections (1.67° < θ < 25.03°). A total of 10522 unique reflections were observed with $I > 2\sigma(I)$ and were used in the calculations.

The structure was solved by direct methods by using SHELXS-97[39] and refined by least-squares procedures. The hydrogen atoms of the water molecules were not added and the other hydrogen atoms were located geometrically and refined isotropically. The final refinement included 811 variable parameters and converged to $R = 0.0750$, $R_w = 0.1612$.

Complexes 2 and 3: The structure determinations of complexes **2** and **3** were similar to that of complex **1**. The grey prism-like crystals of the two complexes, respectively, were used for X-ray data collection. The unit constants were determined from 25 reflections [1.66° < θ < 26.44° (**2**), 1.63° < θ < 25.03° (**3**)].

A total of 13938 (**2**) and 11901 (**3**) unique reflections were observed with $I > 2\sigma(I)$ and were used in the calculations. The final refinement included 809 variable parameters for complex **2** and 886 for complex **3** and converged to $R = 0.0596$, $R_w = 0.1155$ (**2**) and $R = 0.1017$, $R_w = 0.2061$ (**3**).

The crystallographic data for **1**, **2** and **3** are listed in Table 4. CCDC-217659 to -217661 contain the supplementary crystallographic data for this paper. These data can be obtained free of charge at www.ccdc.cam.ac.uk/conts/retrieving.html [or from the Cambridge Crystallographic Data Centre, 12 Union Road, Cambridge CB2 1EZ, UK; Fax: (internat.) +44-1223-336-033; E-mail: deposit@ccdc.cam.ac.uk].

Acknowledgments

This work was supported by the National Science Foundation of China (Grant No.59973008 and 20071019) and the Natural Science Foundation of Tianjin (Grant No. No.013603711).

---

[1] O. Kahn, *Adv. Inorg. Chem.* **1996**, 179.
[2] N. B. O'Bryan, T. O. Marier, I. C. Paul, R. S. Drago, *J. Am. Chem. Soc.* **1973**, *95*, 6640−6645.
[3] J. P. Costes, J. P. Laurent, J. M. M. Sanchez, J. S. Varela, M. Ahlgren, M. Sundberg, *Inorg. Chem.* **1997**, *36*, 4641−4646.
[4] O. Kahn, Y. Pei, M. Verdaguer, J. P. Renard, J. Sletten, *J. Am. Chem. Soc.* **1988**, *110*, 782−789.
[5] H. Okawa, Y. Kawahara, M. Mikuriya, S. Kida, *Bull. Chem. Soc., Jpn.* **1980**, *53*, 549−550.
[6] J. Ribas, C. Diaz, R. Costa, Y. Journaux, C. Mathoniere, O. Kahn, A. Gleizes, *Inorg. Chem.* **1990**, *29*, 2042−2047.
[7] J. C. Livermore, R. D. Willett, R. M. Gaura, C. P. Landee, *Inorg. Chem.* **1982**, *21*, 1403−1405.
[8] M. F. Charlot, S. Jeannin, Y. Jeannin, O. Kahn, J. Lucrèce-Abaul, J. Martin Frere, *Inorg. Chem.* **1979**, *18*, 1675−1681.
[9] M. A. S. Goher, F. A. Mautner, *J. Chem. Soc., Dalton Trans.* **1999**, 1923−1924.

[10] E. Q. Gao, Q. H. Zhao, J. K. Tang, D. Z. Liao, Z. H. Jiang, S. P. Yan, *J. Chem. Soc., Dalton Trans.* **2001**, 1537−1540.

[11] T. S. Billson, J. D. Crane, O. D. Fox, S. L. Heath, *Inorg. Chem. Commun.* **2000**, *3*, 718−720.

[12] L. Zhang, S. B. Wang, G. M. Yang, J. K. Tang, D. Z. Liao, Z. H. Jiang, S. P. Yan, P. Chen, *Inorg. Chem.* **2003**, *42*, 1462−1466.

[13] C. Diaz, J. Ribas, R. Costa, J. Tercero, M. S. E. Fallah, X. Solans, M. Font-Boadía, *Eur. J. Inorg. Chem.* **2000**, *4*, 675−681.

[14] Y. Pei, Y. Joumaux, O. Kahn, *Inorg. Chem.* **1989**, *28*, 100−103.

[15] L. Soto, J. Garcia, E. Escriva, J.-P. Legros, J.-P. Tuchagues, F. Dahan, A. Fuertes, *Inorg. Chem.* **1989**, *28*, 3378−3386.

[16] F. Loret, Y. Journaux, M. Julve, *Inorg. Chem.* **1990**, *29*, 3967−3972.

[17] J. Larionova, S. A. Chavan, J. V. Yakhmi, A. G. Froystein, J. Sletten, C. Sourisseau, O. Kahn, *Inorg. Chem.* **1997**, *36*, 6374−6381.

[18] G. Brewer, C. T. Brewer, P. Kamaras, S. Prytkov, M. Y. Shang, W. R. Scheidt, *Inorg. Chim. Acta* **2001**, *321*, 175−180.

[19] E. Q. Gao, J. K. Tang, S. P. Yan, D. Z. Liao, Z. H. Jiang, *Trans. Met. Chem.* **2001**, *26*, 473−476.

[20] E. Q. Gao, D. Z. Liao, Z. H. Jiang, S. P. Yan, *Polyhedron* **2001**, *20*, 923−927.

[21] E. Q. Gao, J. K. Tang, D. Z. Liao, Z. H. Jiang, S. P. Yan, G. L. Wang, *Helv. Chim. Acta* **2001**, *84*, 908−917.

[22] E. Q. Gao, G.-M. Yang, J. K. Tang, D. Z. Liao, Z. H. Jiang, S. P. Yan, *Polyhedron* **1999**, *18*, 3643−3646.

[23] J. K. Tang, L.-Y. Wang, L. Zhang, E.-Q. Gao, D. Z. Liao, Z. H. Jiang, S. P. Yan, P. Cheng, *Dalton Trans.* **2002**, 1607−1612.

[24] J. K. Tang, Q. L. Wang, E. Q. Gao, J. J. Chen, D. Z. Liao, Z. H. Jiang, S. P. Yan, P. Cheng, *Helv. Chim. Acta* **2002**, *85*, 175−182.

[25] E. Q. Gao, W. M. Bu, G. M. Yang, D. Z. Liao, Z. H. Jiang, S. P. Yan, G. L. Wang, *J. Chem. Soc., Dalton Trans.* **2000**, 1431−1436.

[26] E. A. Vinogradova, O. Y. Vassilyeva, V. N. Kokozay, B.W. Skelton, J. K. Bjernemosee, P. R. Raithby, *Dalton Trans.* **2002**, 4248−4252.

[27] M. Murugesu, R. Clerac, B. Pilawa, A. Mandel, C. E. Anson, A. K. Powell, *Inorg. Chim. Acta* **2002**, *337*, 328−336.

[28] L. H. Yin, W. H. Gu, P. Cheng, L. Z. Zhang, Z. Liao, J. Li, X. L. Yang, X. Q. Fu, S. P. Yan, *Eur. J. Inorg. Chem.* **2002**, *8*, 1937−1940.

[29] E. Colacio, C. Lopez-Magana, V. McKee, A. Romerosa, *J. Chem. Soc., Dalton Trans.* **1999**, 2923−2926.

[30] D. J. Brauer, G. Hessler, P. C. Knuppel, O. Stelzer, *Inorg. Chem.* **1990**, *29*, 2370−2375.

[31] D. Coucouvanis, S. Kanodia, D. Swenson, S.-J. Chen, T. Stüdemann, N. C. Baeziger, R. Pedelty, M. Chu, *J. Am. Chem. Soc.* **1993**, *115*, 11271−11278.

[32] J. Dai, M. Munakata, Y. Ohno, G.-Q. Bian, Y. Suenaga, *Inorg. Chim. Acta* **1999**, *285*, 332−335.

[33] [33a] M. Julve, M. Verdaguer, O. Kahn, A. Gleizes, M. Philoche-levisalles, *Inorg. Chem.* **1983**, *22*, 368−370. [33b] O. Kahn, *Molecular Magnetism,* VCH, New York, **1993**.

[34] E. Q. Gao, H. Y. Sun, D. Z. Liao, Z.H. Jiang, S. P. Yan, *Polyhedron* **2002**, *21*, 359−364.

[35] M. M. Miao, D. Z. Liao, Z. H. Jiang, S. P. Yan, G. L. Wang, *Polyhedron* **1995**, *14*, 1577−1580.

[36] S.W. Bi, C. B. Liu, H. Q. Hu, *J. Phys. Chem. B* **2002**, *106*, 10786−10792.

[37] D. Z. Liao, Q. H. Zhao, Z. Y. Zhang, G. L. Wang, *Trans. Met. Chem.* **1991**, *16*, 209−211.

[38] O. Kahn, *Angew. Chem. Int. Ed. Engl.* **1985**, 24, 834−850.

[39] L. I. Smith, J. W. Opie, *Organic Syntheses*; Wiley: New York, **1995**: Collect. Vol. 3. P. 56.

[40] G. M.Sheldrick, *SHELXS*-97 and *SHELXL*-97, *Software for Crystal Structure Analysis*, Siemens Analytical X-ray Instruments Inc., Madison, WI, USA, **1997**.

Received March 29, 2004
Early View Article